



## Short communication

## Synthesis, molecular modeling and biological evaluation of chalcone thiosemicarbazide derivatives as novel anticancer agents

Hong-Jia Zhang, Yong Qian, Di-Di Zhu, Xu-Guang Yang, Hai-Liang Zhu\*

State Key Laboratory of Pharmaceutical Biotechnology, Nanjing University, Nanjing 210093, People's Republic of China

## ARTICLE INFO

## Article history:

Received 29 January 2011

Received in revised form

24 May 2011

Accepted 9 July 2011

Available online 3 August 2011

## Keywords:

Chalcone

Thiosemicarbazide

Antiproliferative

EGFR

## ABSTRACT

A series of novel chalcone thiosemicarbazide derivatives (**4a–4x**) have been designed, synthesized, structurally determined, and their biological activities were also evaluated as potential EGFR kinase inhibitors. All the synthesized compounds are first reported. Among the compounds, compound **4r** showed the most potent biological activity ( $IC_{50} = 0.78 \pm 0.05 \mu\text{M}$  for HepG2 and  $IC_{50} = 0.35 \mu\text{M}$  for EGFR), which is comparable to the positive controls. Docking simulation was also performed to position compound **4r** into the EGFR active site to determine the probable binding model. Antiproliferative assay results demonstrated that some of these compounds possessed good antiproliferative activity against HepG2. Compound **4r** with potent inhibitory activity in tumor growth inhibition may be a potential anticancer agent.

Crown Copyright © 2011 Published by Elsevier Masson SAS. All rights reserved.

## 1. Introduction

The hepatocellular carcinoma (HCC) is the most often seen histological type of primary liver carcinoma and is one of the cancer types of highest incidence in the world [1]. Most patients diagnosed with HCC have low recovery rates, and conventional and modified therapies currently available are rarely beneficial [2]. The human hepatoma cell line HepG2, established in 1979, is the best-characterized and most frequently used cell line with respect to hepatotoxic endpoints and has been used to examine various mechanisms of hepatotoxicity. The evaluation of multiple endpoints on HepG2 cells allows the prediction of human hepatotoxicity with more than 80% sensitivity and 90% specificity [3]. Therefore, the idea that HepG2 cells can predict overall hepatotoxicity using hepatospecific endpoints is becoming more and more accepted.

Angiogenesis has been intensely investigated as an attractive cancer therapeutic target during the last decade, as angiogenesis is the first rate-limiting step for tumor cells to metastasize and is also essential for cancer growth [4]. The rapid progression of this field is that some important receptors involved in angiogenesis have been identified, including vascular endothelial growth factor receptor (VEGFR), epidermal growth factor receptor

(EGFR) and several others. These growth factor receptor kinases play important roles in the development, progression, aggressiveness and metastasis of many solid tumors, such as non-small cell lung cancer [5], head and neck cancers [6], and glioblastomas [7]. Among these kinases, EGFR (also known as erbB-1 or HER-1) has been implicated in as being significant in cancer. Erlotinib inhibits EGFR that is overexpressed in tumors and is approved antitumor agent [8]. Thus, these factors are important targets for the development of new therapeutic antitumor agents [9,10].

Chalcones (1,3-diaryl-2-propen-1-ones) constitute an important class of natural products belonging to the flavonoid family, which display interesting biological activities including anti-inflammatory [11], antibacterial [12], antioxidant [13], antimarial [14] and anticancer [15]. Due to their abundance in plants and ease of synthesis, this class of compounds has generated great interest for possible therapeutic uses. They are also effective *in vivo* as cell proliferating inhibitors, antitumor promoting and chemopreventing agents [16]. Meanwhile, the anticancer activity of various chalcone molecules has been studied and chalcone with a trimethoxyphenyl unit has been reported to be the most cytotoxic ( $IC_{50} = 0.21 \text{ nM}$ ) derivatives synthesized so far [17] (Fig. 1). O. Sabzevari and coworkers reported that some hydroxylated chalcones showed effective at collapsing the mitochondrial membrane potential which suggests that the cytotoxic activity of hydroxyl chalcones are likely because of their ability to uncouple mitochondria [18]. Since a number of clinically useful anticancer

\* Corresponding author. Tel.: +86 25 8359 2572; fax: +86 25 8359 2672.

E-mail address: [zhuhl@nju.edu.cn](mailto:zhuhl@nju.edu.cn) (H.-L. Zhu).

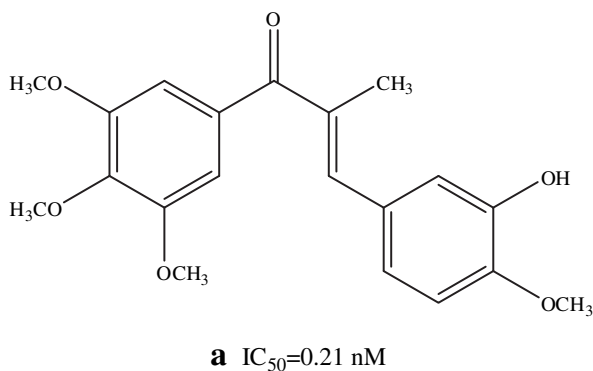


**Fig. 1.** The structure of chalcone with a trimethoxyphenyl unit (**a**).

drugs have genotoxic effects due to interaction with the amino groups of nucleic acids, chalcones may be devoid of this important side effect.

Thiosemicarbazone, a large group of thiourea derivatives, exhibits various biological activities and have therefore attracted considerable pharmaceutical interest [19]. They have been evaluated as antiviral, antibacterial and anticancer therapeutics over the last 50 years, whose biological activities are a function of parent aldehyde or ketone moiety [20]. Conjugated N–N–S tridentate ligand system of thiosemicarbazide ( $NH_2$ –CS–NH– $NH_2$ ) seems essential for anticancer activity [21].

Recently, several kinds of thiosemicarbazone derivatives have been synthesized and their antitumor activities were also reported [21]. But there were few literatures reported for chalcone thiosemicarbazone derivatives and their bioactivity against HCC have not been investigated. With the aim of searching for new pharmaceuticals against HCC, we designed and synthesized a series of chalcone thiosemicarbazone derivatives and examined their activity against the HepG2 cell line.

As a part of our research for novel antitumor agents, we designed and synthesized a series of thiosemicarbazone analogues based on chalcone scaffold, and the biological activity evaluation indicated that some of these compounds are potent inhibitors of EGFR. Docking simulations were performed using the X-ray crystallographic structure of the EGFR in complex with an inhibitor to explore the binding modes of these compounds at the active site.

## 2. Results and discussion

### 2.1. Chemistry

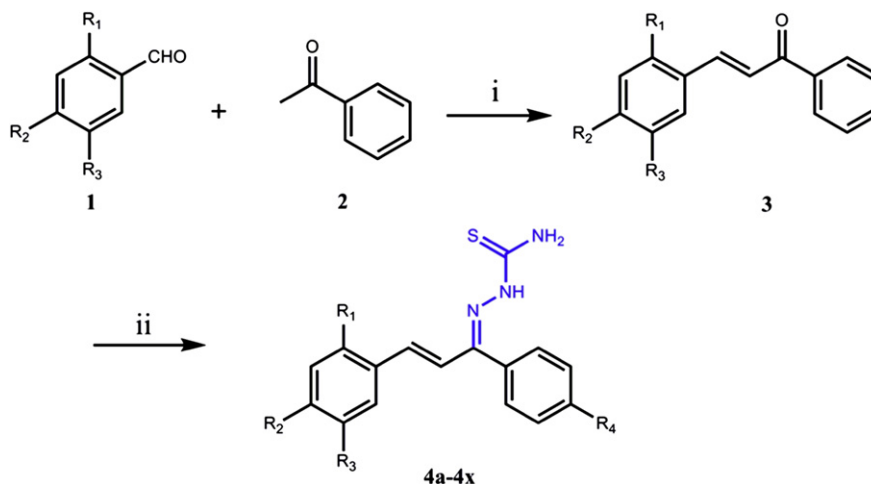
The synthetic route for the novel chalcone thiosemicarbazone derivatives **4a–4x** is outlined in Scheme 1. These compounds were synthesized from the start chalcone and thiosemicarbazide. In our study, chalcone and thiosemicarbazide were dissolved in a mixture of ethanol and acetic acid and refluxed for 24 h at 80 °C, and chalcone thiosemicarbazide derivatives were obtained with yields of 75–85% (**4a–4x**) (Table 1). All of the synthetic compounds gave satisfactory analytical and spectroscopic data, which were in full accordance with their depicted structures.

### 2.2. Biological activity

#### 2.2.1. Antiproliferation assay

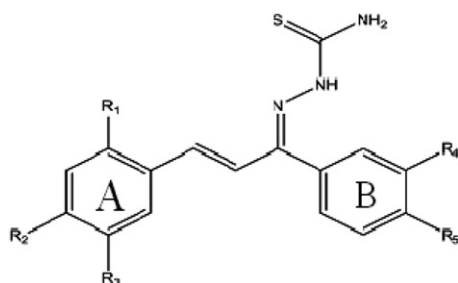
All the synthesized thiosemicarbazide compounds **4a–4x** were evaluated for their ability to antiproliferative activities against human hepatocellular liver carcinoma (HepG2) cell. The results were summarized in Table 2. A number of thiosemicarbazide compounds exhibited remarked effects on antiproliferative activities. Among them, compound **4r** displayed the most potent inhibitory activity ( $IC_{50} = 0.78 \pm 0.05$   $\mu$ M for HepG2), a little decline compared to the positive control Erlotinib ( $IC_{50} = 0.08 \pm 0.005$   $\mu$ M for HepG2).

Structure-activity relationships in these thiosemicarbazide derivatives demonstrated that compounds with substitution at the *meta* (**4e–4g**) position showed more potent activities than those with substitution at the *ortho* (**4a–4d**) and *para* (**4h–4o**) position in the A-ring. A comparison of the *meta* position substitution on the A-ring demonstrated that a *meta* halogen (**4e**) have slightly improved antiproliferative activity. However, a significant loss of activity was observed when the halogen substituent was moved from the *meta* position to the *ortho* (**4a–4c**) or *para* (**4h–4j**) position in the A-ring. Analysis the *para* position substitution on the A-ring, we discovered that a *para* nitro and benzyloxy group could obviously improved antiproliferative activity. A methoxy group at *ortho* (**4d**), *meta* (**4f**), and *para* (**4l**) in the A-ring all led to a noteworthy poor activity. Moreover, aromatic A-ring with a naphthyl moiety substituent (**4x**) exhibited good antiproliferative activity. The compounds with *para* methyl and halogen substituted (**4r**, **4t**) in the B-ring exhibited excellent antiproliferative activity, **4r** with substituent of *p*-Me



**Scheme 1.** General synthesis of chalcone thiosemicarbazide derivatives (**4a–4x**). Reagents and conditions: (i), KOH, MeOH, rt; (ii), thiosemicarbazide, EtOH, AcOH, reflux.

**Table 1**  
Structure of chalcone thiosemicarbazide derivatives (**4a–4x**).



| compd     | R <sub>1</sub> | R <sub>2</sub>      | R <sub>3</sub>  | R <sub>4</sub> | R <sub>5</sub> |
|-----------|----------------|---------------------|-----------------|----------------|----------------|
| <b>4a</b> | F              | H                   | H               | H              | H              |
| <b>4b</b> | Cl             | H                   | H               | H              | H              |
| <b>4c</b> | Br             | H                   | H               | H              | H              |
| <b>4d</b> | OMe            | H                   | H               | H              | H              |
| <b>4e</b> | H              | H                   | F               | H              | H              |
| <b>4f</b> | H              | H                   | OMe             | H              | H              |
| <b>4g</b> | H              | H                   | NO <sub>2</sub> | H              | H              |
| <b>4h</b> | H              | F                   | H               | H              | H              |
| <b>4i</b> | H              | Cl                  | H               | H              | H              |
| <b>4j</b> | H              | Br                  | H               | H              | H              |
| <b>4k</b> | H              | Me                  | H               | H              | H              |
| <b>4l</b> | H              | OMe                 | H               | H              | H              |
| <b>4m</b> | H              | NO <sub>2</sub>     | H               | H              | H              |
| <b>4n</b> | H              | Ph                  | H               | H              | H              |
| <b>4o</b> | H              | OCH <sub>2</sub> Ph | H               | H              | H              |
| <b>4p</b> | H              | H                   | H               | H              | H              |
| <b>4q</b> | H              | H                   | H               | H              | Br             |
| <b>4r</b> | H              | H                   | H               | H              | Me             |
| <b>4s</b> | H              | H                   | H               | H              | OMe            |
| <b>4t</b> | H              | H                   | H               | H              | Cl             |
| <b>4u</b> | H              | H                   | H               | Cl             | Cl             |
| <b>4v</b> | H              | F                   | H               | H              | Br             |
| <b>4w</b> | Cl             | H                   | H               | H              | OMe            |
| <b>4x</b> | A Ring =       |                     | H               | H              | H              |

showed the most potent activity in these compound. However, compound **4q** (*p*-Br) displayed a poor activity. Moreover, for the compound with substitution of two chlorides (**4u**) in the B-ring, the activity was greatly decreased compared with single chlorides (**4t**).

### 2.2.2. EGFR inhibitory assay

The EGFR inhibitory potency of the chalcone thiosemicarbazide derivatives were examined and the results are summarized in Table 2. Most of the tested compounds displayed potent EGFR inhibitory. Among them, compound **4r** condensing by chalcone with *p*-substituted methyl group at B ring and thiosemicarbazide showed the most potent inhibitory with IC<sub>50</sub> of 0.35 μM. This result supported the potent anticancer activity of **4r**. The results of EGFR inhibitory activity of the tested compounds were corresponding to the structure relationships (SAR) of their anticancer activities. This demonstrated that the potent anticancer activities of the synthetic compounds were probably correlated to their EGFR inhibitory activities.

### 2.2.3. Apoptosis assay

In addition, apoptosis is an essential mechanism used to eliminate activated HepG2 cells during the shut down process of excess immune responses and maintain proper immune

homeostasis, while deficient apoptosis of activated HepG2 cells is associated with a wide variety of immune disorders. As a representative of these chalcone thiosemicarbazide derivatives, compound **4r** has been under investigations in vitro experiment. We detected the mechanism of compound **4r** inhibition effects by flow cytometry (FCM) (Fig. 2), and found that the compound could induce the apoptosis of activated HepG2 cells in a dose dependent manner. As shown in Fig. 2, HepG2 cells were treated with 4, 6 and 8 μM of compound **4r** for 18 h. The compound increased the percentage of apoptosis by Annexin V-FITC/PI staining in a dose-dependent manner. The result indicated that compound **4r** induced apoptosis of anticancer stimulated HepG2 cells.

## 3. Conclusions

A series of chalcone-type thiosemicarbazide compounds have been designed and synthesized, and their biological activities were also evaluated as potent anticancer polymerization inhibitors and antiproliferative activity against human hepatocellular liver carcinoma (HepG2) cell. Compound **4r** demonstrated the most potent inhibitory activity that inhibited the growth of HepG2 cells with IC<sub>50</sub> of 0.78 ± 0.05 μM and inhibited the activity of EGFR kinase with IC<sub>50</sub> of 0.35 μM, which was a little decline compared to the positive control erlotinib.

In order to gain more understanding of the structure-activity relationships observed at the EGFR, molecular docking of the most potent inhibitor **4r** into ATP binding site of EGFR kinase was performed on the binding model based on the EGFR complex structure. The binding model of compound **4r** and EGFR is depicted in Fig. 3A and B. Analysis of the compound **4r**'s binding conformation in the colchicine binding site demonstrated that compound **4r** was stabilized by hydrogen bonding interaction with GLN 767 and a cation-π interaction between benzene ring and nitrogen atom of LYS 828. Antiproliferative and apoptosis assay results showed the compound **4r** was a potential anticancer agent.

**Table 2**  
The antiproliferative effect of the compound **4a–4x** against HepG2.

| Compound         | HepG2 IC <sub>50</sub> ± SD(μM) | EGFR inhibition IC <sub>50</sub> (μM) |
|------------------|---------------------------------|---------------------------------------|
| <b>4a</b>        | 14 ± 4                          | 22.36                                 |
| <b>4b</b>        | 16 ± 3                          | 23.27                                 |
| <b>4c</b>        | 17 ± 2                          | 26                                    |
| <b>4d</b>        | 20 ± 3                          | 33                                    |
| <b>4e</b>        | 1.11 ± 0.77                     | 2.08                                  |
| <b>4f</b>        | 5.53 ± 0.3                      | 10.95                                 |
| <b>4g</b>        | 2.64 ± 0.23                     | 3.74                                  |
| <b>4h</b>        | 12 ± 2                          | 19.12                                 |
| <b>4i</b>        | 13 ± 3                          | 20.48                                 |
| <b>4j</b>        | 18 ± 3                          | 26.56                                 |
| <b>4k</b>        | 11 ± 2                          | 17.39                                 |
| <b>4l</b>        | 10 ± 2                          | 14.83                                 |
| <b>4m</b>        | 1.05 ± 0.69                     | 1.57                                  |
| <b>4n</b>        | 2.57 ± 0.15                     | 5.11                                  |
| <b>4o</b>        | 0.85 ± 0.08                     | 0.70                                  |
| <b>4p</b>        | 1.46 ± 0.8                      | 2.38                                  |
| <b>4q</b>        | 6.35 ± 0.34                     | 12.24                                 |
| <b>4r</b>        | 0.78 ± 0.05                     | 0.35                                  |
| <b>4s</b>        | 4.38 ± 0.21                     | 8.66                                  |
| <b>4t</b>        | 0.83 ± 0.07                     | 0.59                                  |
| <b>4u</b>        | 5.16 ± 0.4                      | 9.78                                  |
| <b>4v</b>        | 1.22 ± 0.92                     | 2.17                                  |
| <b>4w</b>        | 3.54 ± 0.26                     | 7.83                                  |
| <b>4x</b>        | 0.81 ± 0.06                     | 0.41                                  |
| <b>Erlotinib</b> | 0.08 ± 0.005                    | 0.03                                  |

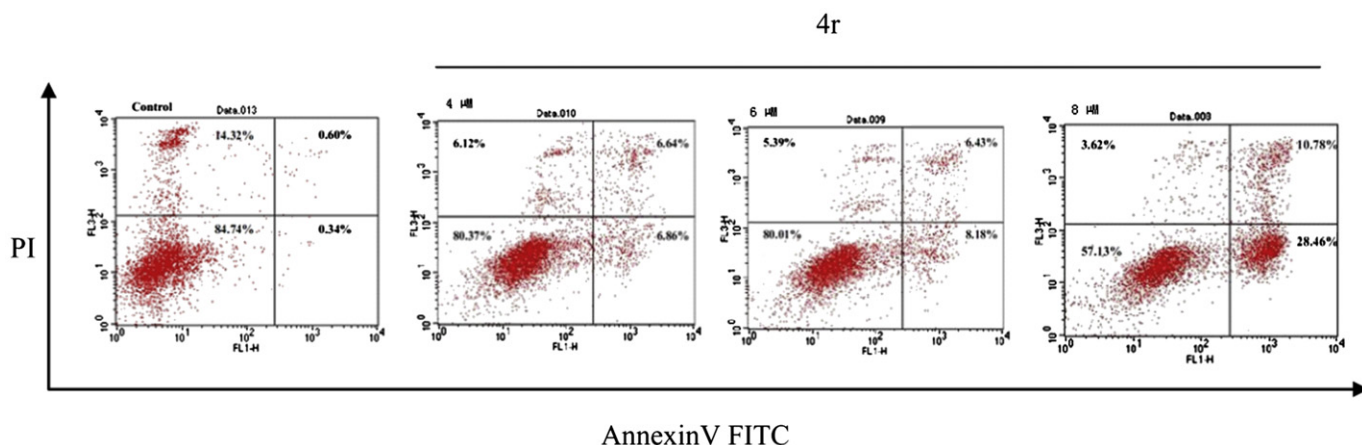


**Fig. 2.** HepG2 cells isolated from naïve mice were cultured with anticancer and various concentrations of **4r** for 18 h. Cells were stained by Annexin V FITC/PI and apoptosis was analyzed by flow cytometry.

## 4. Experimental protocols

### 4.1. Materials and measurements

All chemicals and reagents used in current study were analytical grade. All the  $^1\text{H}$  NMR spectra were recorded on a Bruker DPX 300

or DRX 500 model Spectrometer in  $\text{DMSO}-d_6$  and chemical shifts were reported in ppm ( $\delta$ ). ESI-MS spectra were recorded on a Mariner System 5304 Mass spectrometer. Elemental analyses were performed on a CHN-O-Rapid instrument. TLC was performed on the glass-backed silica gel sheets (silica gel 60 Å GF254) and visualized in UV light (254 nm). Column chromatography was performed using silica gel (200–300 mesh) eluting with ethyl acetate and petroleum ether (ethyl acetate: petroleum ether = 1:3).

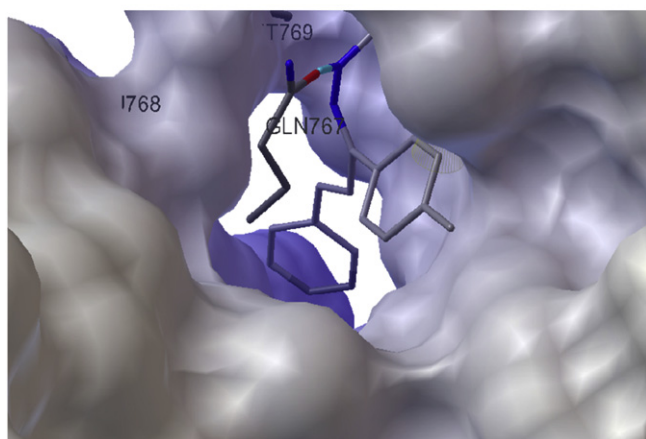
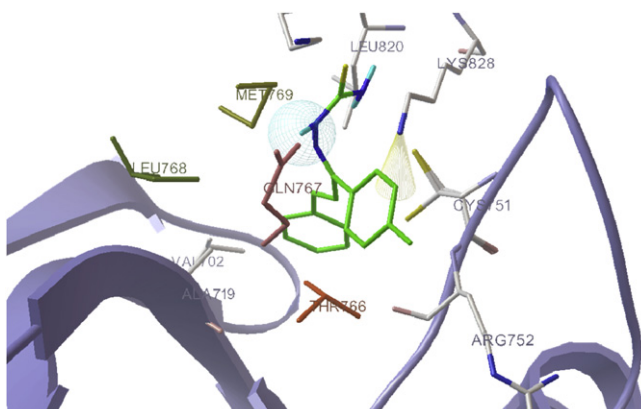


**Fig. 3.** A. Docking of compound **4r** (Carbon atoms are green, nitrogen atoms are dark blue and hydrogen atoms are light blue) with EGFR Kinase shows intermolecular hydrogen bonds with GLN 767 and a cation- $\pi$  interaction between benzene ring and nitrogen atom of LYS 828. B. 3D model of the interaction between compound **4r** and the colchicine binding site. The protein is represented by molecular surface. **4r** is depicted by sticks and balls. (For interpretation of the references to colour in this figure legend, the reader is referred to the web version of this article.)

### 4.2. General procedure for synthesis of chalcones

To a stirred solution of acetophenone derivatives or acetone (1 mmol) and a benzaldehyde derivatives (1 mmol) in MeOH (30 mL) was added 6 M KOH (4 mL) and the reaction mixture was stirred until the solids formed. The products were filtrated and washed carefully with ice water and cool MeOH; the resulting chalcones were purified by crystallization from MeOH in refrigerator (Scheme 1).

### 4.3. General procedure for synthesis of thiosemicarbazide derivatives of chalcone

Equimolar amount of chalcone (0.5 mmol) and thiosemicarbazide (0.5 mmol) were dissolved in ethanol, and acetic acid (250  $\mu\text{L}$ ) as a catalyst and stirred 80  $^\circ\text{C}$  for 24 h. The reaction mixture was concentrated. The product was obtained after purification by column chromatography on silica gel (ethyl acetate: petroleum ether = 1:3). (Scheme 1)

#### 4.3.1. (Z)-2-((E)-3-(2-fluorophenyl)-1-phenylallylidene)hydrazinecarbothioamide (**4a**)

$^1\text{H}$  NMR (300 MHz,  $\text{DMSO}-d_6$ ,  $\delta$  ppm): 7.10 (d,  $J$  = 15.9 Hz, 1H), 7.22 (d,  $J$  = 16.2 Hz, 1H), 7.64–7.67 (m, 5H), 7.81 (d,  $J$  = 15.9 Hz, 4H), 8.23 (d,  $J$  = 6.0 Hz, 1H), 8.34 (s, 1H), 8.62 (s, 1H). ESI-MS: 300.1 ( $\text{C}_{16}\text{H}_{15}\text{FN}_3\text{S}$ ,  $[\text{M} + \text{H}]^+$ ). Anal. Calcd for  $\text{C}_{16}\text{H}_{14}\text{FN}_3\text{S}$ : C, 64.19%; H, 4.71%; N, 14.04%. Found: C, 64.53%; H, 5.06%; N, 14.37%.

#### 4.3.2. (Z)-2-((E)-3-(2-chlorophenyl)-1-phenylallylidene)hydrazinecarbothioamide (**4b**)

$^1\text{H}$  NMR (300 MHz,  $\text{DMSO}-d_6$ ,  $\delta$  ppm): 5.50 (d,  $J$  = 8.1 Hz, 1H), 7.0–7.16 (m, 2H), 7.32–7.52 (m, 7H), 7.98 (d,  $J$  = 16.1 Hz, 2H), 8.56 (s, 2H,  $\text{NH}_2$ ). ESI-MS: 317.1 ( $\text{C}_{16}\text{H}_{15}\text{ClN}_3\text{S}$ ,  $[\text{M} + \text{H}]^+$ ). Anal. Calcd for  $\text{C}_{16}\text{H}_{14}\text{ClN}_3\text{S}$ : C, 60.85%; H, 4.47%; N, 13.31%. Found: C, 61.19%; H, 4.81%; N, 13.67%.

4.3.3. (Z)-2-((E)-3-(2-bromophenyl)-1-phenylallylidene)hydrazine carbothioamide (**4c**)

<sup>1</sup>H NMR (300 MHz, DMSO-*d*<sub>6</sub>, δ ppm): 2.50 (s, 1H), 3.32 (s, 1H), 6.39 (d, *J* = 16.5 Hz, 1H), 6.86 (d, *J* = 16.3 Hz, 1H), 7.19 (d, *J* = 16.4 Hz, 1H), 7.36 (d, *J* = 7.5 Hz, 1H), 7.42–7.50 (m, 2H), 7.55–7.76 (m, 6H). ESI-MS: 361.0 (C<sub>16</sub>H<sub>15</sub>BrN<sub>3</sub>S, [M + H]<sup>+</sup>). Anal. Calcd for C<sub>16</sub>H<sub>14</sub>BrN<sub>3</sub>S: C, 53.34%; H, 3.92%; N, 11.66%. Found: C, 53.68%; H, 4.30%; N, 11.99%.

4.3.4. (Z)-2-((E)-3-(2-methoxyphenyl)-1-phenylallylidene)hydrazinecarbothioamide (**4d**)

<sup>1</sup>H NMR (300 MHz, DMSO-*d*<sub>6</sub>, δ ppm): 3.43 (s, 3H, OCH<sub>3</sub>), 3.83 (s, 2H), 6.06 (dd, *J*<sub>1</sub> = 3.1 Hz, *J*<sub>2</sub> = 3.3 Hz, 1H), 6.80–6.88 (m, 2H), 7.03 (d, *J* = 8.0 Hz, 1H), 7.22 (t, *J* = 8.6 Hz, 1H), 7.43 (d, *J* = 6.3 Hz, 3H), 7.86 (dd, *J*<sub>1</sub> = 2.5 Hz, *J*<sub>2</sub> = 1.6 Hz, 3H), 8.02 (s, 1H, NH). ESI-MS: 312.1 (C<sub>17</sub>H<sub>18</sub>N<sub>3</sub>OS, [M + H]<sup>+</sup>). Anal. Calcd for C<sub>17</sub>H<sub>17</sub>N<sub>3</sub>OS: C, 65.57%; H, 5.50%; N, 13.49%. Found: C, 65.92%; H, 5.83%; N, 13.85%.

4.3.5. (Z)-2-((E)-3-(3-fluorophenyl)-1-phenylallylidene)hydrazinecarbothioamide (**4e**)

<sup>1</sup>H NMR (300 MHz, DMSO-*d*<sub>6</sub>, δ ppm): 2.50 (s, 1H), 3.31 (s, 1H), 7.50–7.98 (m, 12H). ESI-MS: 300.1 (C<sub>16</sub>H<sub>15</sub>FN<sub>3</sub>S, [M + H]<sup>+</sup>). Anal. Calcd for C<sub>16</sub>H<sub>14</sub>FN<sub>3</sub>S: C, 64.19%; H, 4.71%; N, 14.04%. Found: C, 64.56%; H, 5.09%; N, 14.39%.

4.3.6. (Z)-2-((E)-3-(3-methoxyphenyl)-1-phenylallylidene)hydrazinecarbothioamide (**4f**)

<sup>1</sup>H NMR (300 MHz, DMSO-*d*<sub>6</sub>, δ ppm): 3.81 (s, 3H, OCH<sub>3</sub>), 3.72–3.40 (m, 1H), 6.75 (d, *J* = 16.1 Hz, 1H), 6.95 (d, *J* = 6.6 Hz, 1H), 7.05 (d, *J* = 7.9 Hz, 1H), 7.30 (s, 3H), 7.45 (s, 3H), 7.61–7.66 (m, 2H), 7.78 (d, *J* = 16.1 Hz, 1H), 8.30 (s, 1H, NH). ESI-MS: 312.1 (C<sub>17</sub>H<sub>18</sub>N<sub>3</sub>OS, [M + H]<sup>+</sup>). Anal. Calcd for C<sub>17</sub>H<sub>17</sub>N<sub>3</sub>OS: C, 65.57%; H, 5.50%; N, 13.49%. Found: C, 65.95%; H, 5.86%; N, 13.83%.

4.3.7. (Z)-2-((E)-3-(3-nitrophenyl)-1-phenylallylidene)hydrazinecarbothioamide (**4g**)

<sup>1</sup>H NMR (300 MHz, DMSO-*d*<sub>6</sub>, δ ppm): 2.52 (s, 1H), 3.31 (s, 1H), 6.60 (d, *J* = 16.5 Hz, 1H), 6.90 (d, *J* = 16.4 Hz, 1H), 7.37 (t, *J* = 9.0 Hz, 2H), 7.45–7.47 (m, 4H), 8.19 (d, *J* = 8.8 Hz, 1H), 8.25 (d, *J* = 9.0 Hz, 2H), 8.37 (s, 1H, NH). ESI-MS: 327.1 (C<sub>16</sub>H<sub>15</sub>N<sub>4</sub>O<sub>2</sub>S, [M + H]<sup>+</sup>). Anal. Calcd for C<sub>16</sub>H<sub>14</sub>N<sub>4</sub>O<sub>2</sub>S: C, 58.88%; H, 4.32%; N, 17.17%. Found: C, 59.26%; H, 4.68%; N, 17.52%.

4.3.8. (Z)-2-((E)-3-(4-fluorophenyl)-1-phenylallylidene)hydrazinecarbothioamide (**4h**)

<sup>1</sup>H NMR (300 MHz, DMSO-*d*<sub>6</sub>, δ ppm): 3.12–3.19 (m, 1H), 3.86–3.96 (m, 1H), 5.93 (dd, *J*<sub>1</sub> = 3.5 Hz, *J*<sub>2</sub> = 3.3 Hz, 1H), 7.10–7.20 (m, 4H), 7.46 (t, *J* = 3.5 Hz, 3H), 7.87–7.90 (m, 3H), 8.05 (s, 1H, NH). ESI-MS: 300.1 (C<sub>16</sub>H<sub>15</sub>FN<sub>3</sub>S, [M + H]<sup>+</sup>). Anal. Calcd for C<sub>16</sub>H<sub>14</sub>FN<sub>3</sub>S: C, 64.19%; H, 4.71%; N, 14.04%. Found: C, 64.44%; H, 5.05%; N, 14.39%.

4.3.9. (Z)-2-((E)-3-(4-chlorophenyl)-1-phenylallylidene)hydrazinecarbothioamide (**4i**)

<sup>1</sup>H NMR (300 MHz, DMSO-*d*<sub>6</sub>, δ ppm): 3.14 (dd, *J*<sub>1</sub> = 3.5 Hz, *J*<sub>2</sub> = 3.5 Hz, 1H), 3.85–3.95 (m, 1H), 5.93 (dd, *J*<sub>1</sub> = 3.3 Hz, *J*<sub>2</sub> = 3.3 Hz, 1H), 7.12 (d, *J* = 7.1 Hz, 2H), 7.20–7.34 (m, 3H), 7.52 (d, *J* = 8.4 Hz, 2H), 7.90 (d, *J* = 8.4 Hz, 2H), 8.00 (d, *J* = 26.7 Hz, 2H). ESI-MS: 317.1 (C<sub>16</sub>H<sub>15</sub>ClN<sub>3</sub>S, [M + H]<sup>+</sup>). Anal. Calcd for C<sub>16</sub>H<sub>14</sub>ClN<sub>3</sub>S: C, 60.85%; H, 4.47%; N, 13.31%. Found: C, 61.21%; H, 4.85%; N, 13.69%.

4.3.10. (Z)-2-((E)-3-(4-bromophenyl)-1-phenylallylidene)hydrazinecarbothioamide (**4j**)

<sup>1</sup>H NMR (300 MHz, DMSO-*d*<sub>6</sub>, δ ppm): 2.50 (s, 1H), 3.60 (s, 1H), 7.37 (t, *J* = 8.2 Hz, 1H), 7.47–7.52 (m, 1H), 7.58 (t, *J* = 7.7 Hz, 2H), 7.66–7.75 (m, 4H), 7.87 (d, *J* = 15.5 Hz, 2H), 7.97 (d, *J* = 15.5 Hz, 1H),

8.16 (d, *J* = 8.6 Hz, 1H). ESI-MS: 361.0 (C<sub>16</sub>H<sub>15</sub>BrN<sub>3</sub>S, [M + H]<sup>+</sup>). Anal. Calcd for C<sub>16</sub>H<sub>14</sub>BrN<sub>3</sub>S: C, 53.34%; H, 3.92%; N, 11.66%. Found: C, 53.69%; H, 4.30%; N, 12.03%.

4.3.11. (Z)-2-((E)-1-phenyl-3-*p*-tolylallylidene)hydrazinecarbothioamide (**4k**)

<sup>1</sup>H NMR (300 MHz, DMSO-*d*<sub>6</sub>, δ ppm): 2.33 (s, 3H, CH<sub>3</sub>), 3.83–3.93 (m, 1H), 5.88 (dd, *J*<sub>1</sub> = 3.1 Hz, *J*<sub>2</sub> = 3.1 Hz, 1H), 7.01 (d, *J* = 8.0 Hz, 2H), 7.11 (d, *J* = 7.9 Hz, 2H), 7.21 (d, *J* = 8.1 Hz, 1H), 7.44–7.46 (m, 3H), 7.86–7.88 (m, 3H), 7.80 (s, 1H, NH). ESI-MS: 296.1 (C<sub>17</sub>H<sub>18</sub>N<sub>3</sub>S, [M + H]<sup>+</sup>). Anal. Calcd for C<sub>17</sub>H<sub>17</sub>N<sub>3</sub>S: C, 69.12%; H, 5.80%; N, 14.22%. Found: C, 69.48%; H, 6.15%; N, 14.58%.

4.3.12. (Z)-2-((E)-3-(4-methoxyphenyl)-1-phenylallylidene)hydrazinecarbothioamide (**4l**)

<sup>1</sup>H NMR (300 MHz, DMSO-*d*<sub>6</sub>, δ ppm): 3.72 (s, 3H, OCH<sub>3</sub>), 3.83–3.92 (m, 1H), 5.87 (dd, *J*<sub>1</sub> = 3.3 Hz, *J*<sub>2</sub> = 3.1 Hz, 1H), 6.87 (d, *J* = 8.6 Hz, 2H), 7.05 (d, *J* = 8.6 Hz, 2H), 7.47 (t, *J* = 3.5 Hz, 3H), 7.98 (s, 1H, NH), 7.87–7.90 (m, 3H). ESI-MS: 312.1 (C<sub>17</sub>H<sub>18</sub>N<sub>3</sub>OS, [M + H]<sup>+</sup>). Anal. Calcd for C<sub>17</sub>H<sub>17</sub>N<sub>3</sub>OS: C, 65.57%; H, 5.50%; N, 13.49%. Found: C, 65.95%; H, 5.86%; N, 13.83%.

4.3.13. (Z)-2-((E)-3-(4-nitrophenyl)-1-phenylallylidene)hydrazinecarbothioamide (**4m**)

<sup>1</sup>H NMR (300 MHz, DMSO-*d*<sub>6</sub>, δ ppm): 6.90 (d, *J* = 16.0 Hz, 1H), 7.65 (d, *J* = 7.0 Hz, 4H), 8.01 (d, *J* = 6.9 Hz, 3H), 8.19–8.27 (m, 5H), 8.38 (s, 1H, NH). ESI-MS: 327.1 (C<sub>16</sub>H<sub>15</sub>N<sub>4</sub>O<sub>2</sub>S, [M + H]<sup>+</sup>). Anal. Calcd for C<sub>16</sub>H<sub>14</sub>N<sub>4</sub>O<sub>2</sub>S: C, 58.88%; H, 4.32%; N, 17.17%. Found: C, 59.26%; H, 4.67%; N, 17.52%.

4.3.14. (Z)-2-((E)-3-(biphenyl-4-yl)-1-phenylallylidene)hydrazinecarbothioamide (**4n**)

<sup>1</sup>H NMR (300 MHz, DMSO-*d*<sub>6</sub>, δ ppm): 3.20 (dd, *J*<sub>1</sub> = 3.1 Hz, *J*<sub>2</sub> = 3.3 Hz, 1H), 3.89–4.04 (m, 1H), 5.75 (s, 1H), 5.98 (d, *J* = 11.3 Hz, 1H), 7.23 (d, *J* = 8.0 Hz, 2H), 7.35 (d, *J* = 7.0 Hz, 1H), 7.45 (t, *J* = 7.3 Hz, 6H), 7.73 (d, *J* = 8.2 Hz, 1H), 7.83 (d, *J* = 7.7 Hz, 1H), 7.89 (t, *J* = 3.8 Hz, 3H), 8.06 (s, 1H, NH). ESI-MS: 358.1 (C<sub>22</sub>H<sub>20</sub>N<sub>3</sub>S, [M + H]<sup>+</sup>). Anal. Calcd for C<sub>22</sub>H<sub>19</sub>N<sub>3</sub>S: C, 73.92%; H, 5.36%; N, 11.75%. Found: C, 74.30%; H, 5.69%; N, 12.08%.

4.3.15. (Z)-2-((E)-3-(4-(benzyloxy)phenyl)-1-phenylallylidene)hydrazinecarbothioamide (**4o**)

<sup>1</sup>H NMR (300 MHz, DMSO-*d*<sub>6</sub>, δ ppm): 3.13 (dd, *J*<sub>1</sub> = 3.1 Hz, *J*<sub>2</sub> = 3.2 Hz, 1H), 3.82–3.92 (m, 1H), 5.06 (s, 2H), 5.84–5.89 (m, 1H), 6.95 (d, *J* = 8.6 Hz, 2H), 7.06 (d, *J* = 8.6 Hz, 2H), 7.29–7.47 (m, 8H), 7.87 (t, *J* = 3.8 Hz, 3H), 7.99 (s, 1H, NH). ESI-MS: 388.1 (C<sub>23</sub>H<sub>22</sub>N<sub>3</sub>OS, [M + H]<sup>+</sup>). Anal. Calcd for C<sub>23</sub>H<sub>21</sub>N<sub>3</sub>OS: C, 71.29%; H, 5.46%; N, 10.84%. Found: C, 71.65%; H, 5.80%; N, 11.19%.

4.3.16. (Z)-2-((E)-1,3-diphenylallylidene)hydrazinecarbothioamide (**4p**)

<sup>1</sup>H NMR (500 MHz, DMSO-*d*<sub>6</sub>, δ ppm): 6.78 (d, *J* = 16.0 Hz, 1H), 7.35–7.43 (m, 3H), 7.45–7.48 (m, 3H), 7.63–7.66 (m, 2H), 7.74 (d, *J* = 7.0 Hz, 2H), 7.80 (s, 1H), 7.81 (d, *J* = 16.0 Hz, 1H), 8.31 (s, 1H), 11.09 (s, 1H). ESI-MS: 282.1 (C<sub>16</sub>H<sub>16</sub>N<sub>3</sub>S, [M + H]<sup>+</sup>). Anal. Calcd for C<sub>16</sub>H<sub>15</sub>N<sub>3</sub>S: C, 68.30%; H, 5.37%; N, 14.93%. Found: C, 68.64%; H, 5.73%; N, 15.31%.

4.3.17. (Z)-2-((E)-1-(4-bromophenyl)-3-phenylallylidene)hydrazinecarbothioamide (**4q**)

<sup>1</sup>H NMR (300 MHz, DMSO-*d*<sub>6</sub>, δ ppm): 3.14 (d, *J* = 18.7 Hz, 1H), 3.85–3.95 (m, 1H), 5.93 (d, *J* = 8.2 Hz, 1H), 7.13 (d, *J* = 7.3 Hz, 2H), 7.24 (d, *J* = 7.9 Hz, 1H), 7.31 (t, *J* = 7.6 Hz, 2H), 7.52 (d, *J* = 8.4 Hz, 2H), 7.90 (d, *J* = 8.4 Hz, 2H), 7.97 (s, 1H), 8.05 (s, 1H, NH). ESI-MS:

361.0 (C<sub>16</sub>H<sub>15</sub>BrN<sub>3</sub>S, [M + H]<sup>+</sup>). Anal. Calcd for C<sub>16</sub>H<sub>14</sub>BrN<sub>3</sub>S: C, 53.34%; H, 3.92%; N, 11.66%. Found: C, 53.69%; H, 4.30%; N, 12.03%.

4.3.18. (Z)-2-((E)-3-phenyl-1-p-tolylallylidene)hydrazinecarbothioamide (**4r**)

<sup>1</sup>H NMR (300 MHz, DMSO-*d*<sub>6</sub>, δ ppm): 2.36 (s, 3H, CH<sub>3</sub>), 3.08 (s, 1H), 3.83–3.93 (m, 1H), 5.61 (s, 1H), 5.95 (dd, *J*<sub>1</sub> = 3.1 Hz, *J*<sub>2</sub> = 3.1 Hz, 1H), 7.16 (d, *J* = 6.9 Hz, 2H), 7.22–7.33 (m, 5H), 7.73 (d, *J* = 8.1 Hz, 2H), 7.88 (s, 1H, NH). ESI-MS: 295.1 (C<sub>17</sub>H<sub>18</sub>N<sub>3</sub>S, [M + H]<sup>+</sup>). Anal. Calcd for C<sub>17</sub>H<sub>17</sub>N<sub>3</sub>S: C, 69.12%; H, 5.80%; N, 14.22%. Found: C, 69.48%; H, 6.17%; N, 14.59%.

4.3.19. (Z)-2-((E)-1-(4-methoxyphenyl)-3-phenylallylidene)hydrazinecarbothioamide (**4s**)

<sup>1</sup>H NMR (300 MHz, DMSO-*d*<sub>6</sub>, δ ppm): 3.83 (s, 3H, OCH<sub>3</sub>), 5.67 (d, *J* = 8.0 Hz, 1H), 6.79 (d, *J* = 7.1 Hz, 1H), 7.0–7.13 (m, 3H), 7.33–7.72 (m, 7H), 8.56 (s, 2H, NH<sub>2</sub>). ESI-MS: 312.1 (C<sub>17</sub>H<sub>18</sub>N<sub>3</sub>OS, [M + H]<sup>+</sup>). Anal. Calcd for C<sub>17</sub>H<sub>17</sub>N<sub>3</sub>OS: C, 65.57%; H, 5.50%; N, 13.49%. Found: C, 65.96%; H, 5.87%; N, 13.88%.

4.3.20. (Z)-2-((E)-1-(4-chlorophenyl)-3-phenylallylidene)hydrazinecarbothioamide (**4t**)

<sup>1</sup>H NMR (300 MHz, DMSO-*d*<sub>6</sub>, δ ppm): 3.13 (d, *J* = 18.3 Hz, 1H), 3.85–3.95 (m, 1H), 5.93 (d, *J* = 8.0 Hz, 1H), 7.13 (d, *J* = 7.1 Hz, 2H), 7.23 (d, *J* = 7.3 Hz, 1H), 7.31 (t, *J* = 7.3 Hz, 2H), 7.52 (d, *J* = 8.4 Hz, 2H), 7.90 (d, *J* = 8.4 Hz, 2H), 7.97 (s, 1H), 8.05 (s, 1H, NH). ESI-MS: 317.1 (C<sub>16</sub>H<sub>15</sub>ClN<sub>3</sub>S, [M + H]<sup>+</sup>). Anal. Calcd for C<sub>16</sub>H<sub>14</sub>ClN<sub>3</sub>S: C, 60.85%; H, 4.47%; N, 13.31%. Found: C, 61.21%; H, 4.75%; N, 13.68%.

4.3.21. (Z)-2-((E)-1-(3,4-dichlorophenyl)-3-phenylallylidene)hydrazinecarbothioamide (**4u**)

<sup>1</sup>H NMR (300 MHz, DMSO-*d*<sub>6</sub>, δ ppm): 5.67 (d, *J* = 8.1 Hz, 1H), 6.79 (d, *J* = 7.2 Hz, 1H), 7.0 (s, 1H), 7.33–7.85 (m, 8H), 8.56 (s, 2H, NH<sub>2</sub>). ESI-MS: 351.0 (C<sub>16</sub>H<sub>14</sub>Cl<sub>2</sub>N<sub>3</sub>S, [M + H]<sup>+</sup>). Anal. Calcd for C<sub>16</sub>H<sub>13</sub>Cl<sub>2</sub>N<sub>3</sub>S: C, 54.86%; H, 3.74%; N, 12.00%. Found: C, 55.24%; H, 4.11%; N, 12.36%.

4.3.22. (Z)-2-((E)-1-(4-bromophenyl)-3-(4-fluorophenyl)allylidene)hydrazinecarbothioamide (**4v**)

<sup>1</sup>H NMR (300 MHz, DMSO-*d*<sub>6</sub>, δ ppm): 3.14 (dd, *J*<sub>1</sub> = 3.3 Hz, *J*<sub>2</sub> = 3.1 Hz, 1H), 3.84–3.94 (m, 1H), 5.92 (dd, *J*<sub>1</sub> = 3.3 Hz, *J*<sub>2</sub> = 3.4 Hz, 1H), 7.10–7.16 (m, 4H), 7.66 (d, *J* = 8.2 Hz, 2H), 8.02 (d, *J* = 30.9 Hz, 2H). ESI-MS: 377.0 (C<sub>16</sub>H<sub>14</sub>BrFN<sub>3</sub>S, [M + H]<sup>+</sup>). Anal. Calcd for C<sub>16</sub>H<sub>13</sub>BrFN<sub>3</sub>S: C, 50.80%; H, 3.46%; N, 11.11%. Found: C, 51.15%; H, 3.80%; N, 11.47%.

4.3.23. (Z)-2-((E)-3-(2-chlorophenyl)-1-(4-methoxyphenyl)allylidene)hydrazinecarbothioamide (**4w**)

<sup>1</sup>H NMR (300 MHz, DMSO-*d*<sub>6</sub>, δ ppm): 3.88 (s, 3H, CH<sub>3</sub>), 6.84 (d, *J* = 13.0 Hz, 1H), 7.09 (d, *J* = 8.8 Hz, 2H), 7.38 (dd, *J*<sub>1</sub> = 8.6 Hz, *J*<sub>2</sub> = 8.6 Hz, 2H), 7.53 (d, *J* = 8.4 Hz, 2H), 7.69 (d, *J* = 15.6 Hz, 1H), 7.92–8.00 (m, 3H), 8.17 (d, *J* = 9.0 Hz, 2H). ESI-MS: 347.1 (C<sub>17</sub>H<sub>17</sub>ClN<sub>3</sub>S, [M + H]<sup>+</sup>). Anal. Calcd for C<sub>17</sub>H<sub>16</sub>ClN<sub>3</sub>S: C, 61.90%; H, 4.89%; N, 12.74%. Found: C, 62.26%; H, 5.27%; N, 13.09%.

4.3.24. (Z)-2-((E)-3-(naphthalen-1-yl)-1-phenylallylidene)hydrazinecarbothioamide (**4x**)

<sup>1</sup>H NMR (300 MHz, DMSO-*d*<sub>6</sub>, δ ppm): 3.07 (dd, *J*<sub>1</sub> = 3.7 Hz, *J*<sub>2</sub> = 3.4 Hz, 1H), 4.10–4.20 (m, 1H), 6.66–6.70 (m, 1H), 7.03 (d, *J* = 7.1 Hz, 1H), 7.54–7.68 (m, 5H), 7.81–7.88 (m, 3H), 7.97–8.04 (m, 4H), 8.35 (d, *J* = 8.4 Hz, 1H). ESI-MS: 332.1 (C<sub>20</sub>H<sub>18</sub>N<sub>3</sub>S, [M + H]<sup>+</sup>). Anal. Calcd for C<sub>20</sub>H<sub>17</sub>N<sub>3</sub>S: C, 72.48%; H, 5.17%; N, 12.68%. Found: C, 72.84%; H, 5.53%; N, 13.03%.

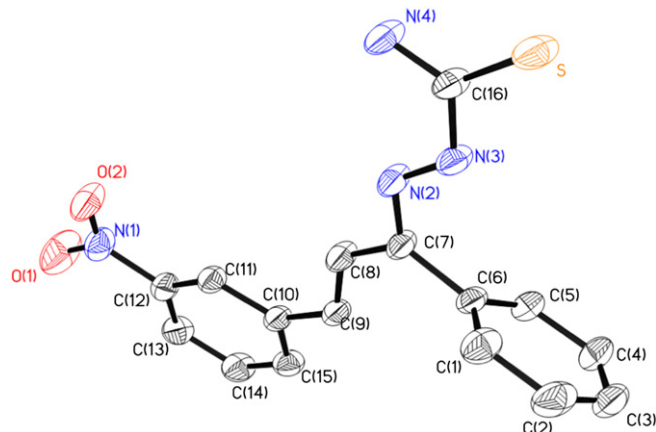


Fig. 4. Crystal structure diagrams of compound **4g**. Molecule structure diagram with displacement ellipsoids being at the 30% probability level and H atoms are shown as small spheres of arbitrary radii.

#### 4.4. Crystal structure determination

Crystal structure determination of compound **4g** were carried out on a Nonius CAD4 diffractometer equipped with graphite-monochromated MoK $\alpha$ ( $\lambda = 0.71073$  ) radiation (Fig. 4). The structure was solved by direct methods and refined on F<sup>2</sup> by full-matrix least-squares methods using SHELX-97 [22]. All the non-hydrogen atoms were refined anisotropically. All the hydrogen atoms were placed in calculated positions and were assigned fixed isotropic thermal parameters at 1.2 times the equivalent isotropic U of the atoms to which they are attached and allowed to ride on their respective parent atoms. The contributions of these hydrogen atoms were included in the structure-factors calculations. The crystal data, data collection, and refinement parameter for the compound **4g** are listed in Table 3. X-ray coordinates have been deposited with the Cambridge Crystallographic Data Centre for small molecules and the CCDC deposition number is 821674.

#### 4.5. General procedure for preparation, purification of EGFR inhibitory assay

A 1.6 kb cDNA encoded for the EGFR cytoplasmic domain (EGFR-CD, amino acids 645–1186) were cloned into baculoviral expression

Table 3  
Crystallographical and experimental data for compound **4g**.

| Compound   | <b>4g</b>  |
|--|--|
| Empirical formula  | C <sub>16</sub> H <sub>14</sub> SN <sub>4</sub> O <sub>2</sub> |
| Formula weight   | 326.08   |
| Crystal system   | Triclinic  |
| Space group  | <i>P</i> -1  |
| <i>a</i> (Å)   | 8.1880(16)   |
| <i>b</i> (Å)   | 8.7080(17)   |
| <i>c</i> (Å)   | 12.088(2)  |
| $\alpha$ (°)   | 91.16(3)   |
| $\beta$ (°)  | 94.46(3)   |
| $\gamma$ (°)   | 108.04(3)  |
| <i>V</i> (Å <sup>3</sup> )   | 816.1(3)   |
| <i>Z</i>   | 11   |
| <i>D</i> <sub>calc</sub> /g cm <sup>-3</sup>   | 1.681  |
| $\theta$ range (°)   | 1.69–25.27   |
| <i>F</i> (000)   | 418  |
| Reflections collected/unique   | 3178/2955 [ <i>R</i> <sub>int</sub> = 0.0151]                  |
| Data/restraints/parameters   | 2955/0/212   |
| Absorption coefficient (mm <sup>-1</sup> )   | 0.804  |
| <i>R</i> <sub>1</sub> ; <i>wR</i> <sub>2</sub> [ <i>I</i> > 2 $\sigma$ ( <i>I</i> )] | 0.0472/0.1270  |
| <i>R</i> <sub>1</sub> ; <i>wR</i> <sub>2</sub> (all data)                            | 0.0674/0.1413  |
| GOOF   | 1.048  |

vectors pBlueBacHis2B and pFASTBacHTc (Huakang Company China), separately. A sequence that encodes (His)<sub>6</sub> was located at the 5' upstream to the EGFR sequences. Sf-9 cells were infected for 3 days for protein expression. Sf-9 cell pellets were solubilized at 0 °C in a buffer at pH 7.4 containing 50 mM HEPES, 10 mM NaCl, 1% Triton, 10 μM ammonium molybdate, 100 μM sodium vanadate, 10 μg/mL aprotinin, 10 μg/mL leupeptin, 10 μg/mL pepstatin, and 16 μg/mL benzamidine HCl for 20 min followed by 20 min centrifugation. Crude extract supernatant was passed through an equilibrated Ni-NTA superflow packed column and washed with 10 mM and then 100 mM imidazole to remove nonspecifically bound material. Histidine tagged proteins were eluted with 250 and 500 mM imidazole and dialyzed against 50 mM NaCl, 20 mM HEPES, 10% glycerol, and 1 μg/mL each of aprotinin, leupeptin, and pepstatin for 2 h. The entire purification procedure was performed at 4 °C or on ice [23].

The EGFR kinase assays was set up to assess the level of autophosphorylation based on DELFIA/Time-Resolved Fluorometry. Compounds **4a–4x** were dissolved in 100% DMSO and diluted to the appropriate concentrations with 25 mM HEPES at pH 7.4. In each well, 10 μL compound was incubated with 10 μL (5 ng for EGFR) recombinant enzyme (1:80 dilution in 100 mM HEPES) for 10 min at room temperature. Then, 10 μL of 5 × buffer (containing 20 mM HEPES, 2 mM MnCl<sub>2</sub>, 100 μM Na<sub>3</sub>VO<sub>4</sub>, and 1 mM DTT) and 20 μL of 0.1 mM ATP-50 mM MgCl<sub>2</sub> were added for 1 h. Positive and negative controls were included in each plate by incubation of enzyme with or without ATP-MgCl<sub>2</sub>. At the end of incubation, liquid was aspirated, and plates were washed three times with wash buffer. A 75 μL (400 ng) sample of europium labeled anti-phosphotyrosine antibody was added to each well for another 1 h of incubation. After washing, enhancement solution was added and the signal was detected by Victor (Wallac Inc.) with excitation at 340 nm and emission at 615 nm. The percentage of autophosphorylation inhibition by the compounds was calculated using the following equation: 100% - [(negative control)/(positive control - negative control)]. The IC<sub>50</sub> was obtained from curves of percentage inhibition with eight concentrations of compound. As the contaminants in the enzyme preparation are fairly low, the majority of the signal detected by the anti-phosphotyrosine antibody is from EGFR.

#### 4.6. Cell proliferation assay

The antiproliferative activities of chalcone thiosemicarbazide derivatives were determined using a standard (MTT)-based colorimetric assay (Sigma). Briefly, cell lines were seeded at a density of 7 × 10<sup>3</sup> cells/well in 96-well microtiter plates (Costar). After 24 h, exponentially growing cells were exposed to the indicated compounds at final concentrations ranging from 0.1 to 40 mg/mL. After 48 h, cell survival was determined by the addition of an MTT solution (20 μL of 5 mg/mL MTT in PBS). After 6 h, 100 μL of 10% SDS in 0.01 N HCl was added, and the plates were incubated at 37 °C for a further 4 h; optical absorbance was measured at 570 nm on an LX300 Epson Diagnostic microplate reader. Survival ratios are expressed in percentages with respect to untreated cells. IC<sub>50</sub> values were determined from replicates of 6 wells from at least two independent experiments.

#### 4.7. Apoptosis assay

HepG2 cells were treated with various concentrations of compound **4r** for 18 h and then stained with both Annexin V-FITC (fluorescein isothiocyanate) and propidium iodide (PI). Then samples were analyzed by FACSCalibur flow cytometer (Becton Dickinson, SanJose, CA).

#### 4.8. Molecular docking modeling

Molecular docking of compound **4r** into the three-dimensional EGFR complex structure (1M17.pdb, downloaded from the PDB) was carried out using the AutoDock software package (version 4.0) as implemented through the graphical user interface Auto-Dock Tool Kit (ADT 1.4.6).

First, AutoGrid component of the program precalculates a three-dimensional grid of interaction energies based on the macromolecular target using the AMBER force field. Then automated docking studies were carried out to evaluate the binding free energy of the inhibitors within the macromolecules. The three-dimensional structures of the aforementioned compounds were constructed using Chem. 3D ultra 11.0 software [Chemical Structure Drawing Standard; Cambridge Soft corporation, USA (2009)], then they were energetically minimized by using MOPAC with 100 iterations and minimum RMS gradient of 0.10. The Gasteiger-Hückel charges of ligands were assigned. The crystal structures of telomerase (PDB code: 1M17) complex were retrieved from the RCSB Protein Data Bank (<http://www.rcsb.org/pdb/home/home.do>). All bound waters and ligands were eliminated from the protein and the polar hydrogens and the Kollman-united charges were added to the proteins.

#### Acknowledgements

This work was supported by Jiangsu National Science Foundation (No. BK2009239).

#### References

- [1] S.P. Dourakis, *Curr. Canc. Ther. Rev.* 4 (2008) 219–226.
- [2] L.C. Chiang, L.T. Ng, I.C. Lin, P.L. Kuo, C.C. Lin, *Canc. Lett.* 37 (2006) 207–214.
- [3] J. Niklas, F. Noor, E. Heinzle, *Toxicol. Appl. Pharmacol.* 240 (2009) 327–336.
- [4] J.M. Cherrington, L.M. Strawn, L.K. Shawver, *Adv. Cancer Res.* 79 (2000) 1–38.
- [5] M. Tateishi, T. Ishida, T. Mitsudomi, S. Kaneko, K. Sugimachi, *Cancer Res.* 50 (1990) 7077–7080.
- [6] T.P. Fleming, A. Saxena, W.C. Clark, J.T. Robertson, E.H. Oldfield, S.A. Aaronson, I.U. Ali, *Cancer Res.* 52 (1992) 4550–4553.
- [7] D.M. Shin, J.Y. Ro, W.K. Hong, W.N. Hittelman, *Cancer Res.* 54 (1994) 3153–3159.
- [8] R.B. Cohen, *Clin. Colorectal Cancer* 2 (2003) 246–251.
- [9] A.L. Gangjee, W. Lin, L. Zeng, Y. Ilnat, M. Warnke, L.A. Green, D.W. Cody, V. Pace, J. Queener, *Bioorg. Med. Chem.* 17 (2009) 7324–7336.
- [10] T.V. Hughes, G. Xu, S.K. Wetter, P.J. Connolly, S.L. Emanuel, P. Karnachi, S.R. Pollack, N. Pandey, M. Adams, M.M. Sandra, S.A. Middleton, L.M. Greenberger, *Bioorg. Med. Chem. Lett.* 18 (2008) 4896–4899.
- [11] J.H. Cheng, C.F. Hung, S.C. Yang, J.P. Wang, S.J. Won, C.N. Lin, *Bioorg. Med. Chem.* 16 (2008) 7270–7276.
- [12] S.F. Nielsen, T. Boesen, M. Larsen, K. Schonning, H. Kromann, *Bioorg. Med. Chem.* 12 (2004) 3047–3054.
- [13] C. Zhan, J. Yang, *Pharmacol. Res.* 53 (2006) 303–309.
- [14] M. Liu, P. Wilairat, M.L. Go, *J. Med. Chem.* 44 (2001) 4443–4452.
- [15] M.L. Go, X. Wu, X.L. Liu, *Curr. Med. Chem.* 12 (2005) 481–499.
- [16] V.S. Koeni, K. Abdhesh, K. Manoj, S. Jayanta, S. Sudhir, *Bioorg. Med. Chem. Lett.* 20 (2010) 7205–7211.
- [17] N.J. Lawrence, D. Rennison, A.T. McGown, J.A. Hadfield, *Bioorg. Med. Chem. Lett.* 13 (2003) 3759–3763.
- [18] O. Sabzevari, G. Galati, M.Y. Moridani, A. Siraki, P.J. O'Brien, *Chem. Biol. Interact* 148 (2004) 57–67.
- [19] W.X. Hu, W. Zhou, C.N. Xia, X. Wen, *Bioorg. Med. Chem. Lett.* 16 (2006) 2213–2218.
- [20] X. Du, C. Guo, E. Hansall, P.S. Doyle, C.R. Caffrey, T.P. Holler, J.H. McKerrow, F.E. Cohen, *J. Med. Chem.* 45 (2002) 2695–2707.
- [21] K. Hu, Z.-J. Yang, S.-S. Pan, H.-J. Xu, J. Ren, *Eur. J. Med. Chem.* 45 (2010) 3453–3458.
- [22] G.M. Sheldrick, SHELX-97, Program for X-ray crystal structure solution and refinement. Göttingen University, Germany, 1997.
- [23] H.R. Tsou, N. Mamuya, B.D. Johnson, M.F. Reich, B.C. Gruber, F. Ye, R. Nilakantan, R. Shen, C. Discafani, R. DeBlanc, R. Davis, F.E. Koehn, L.M. Greenberger, Y.F. Wang, A. Wissner, *J. Med. Chem.* 44 (2001) 2719–2734.